Renewable and Sustainable Energy Reviews 104 (2019) 492–503

Contents lists available at ScienceDirect

Renewable and Sustainable Energy Reviews

journal homepage: www.elsevier.com/locate/rser

Co-located deployment of offshore wind turbines with tidal stream turbine arrays for improved cost of electricity generation

D. Lande-Sudall[a,*], T. Stallard[b], P. Stansby[b]

[a] Western Norway University of Applied Sciences, Department of Mechanical and Marine Engineering, Inndalsveien 28, 5063 Bergen, Norway
[b] University of Manchester, School of Mechanical, Aerospace and Civil Engineering, Oxford Road, Manchester M13 9PL, UK

ARTICLE INFO

Keywords:
Co-location
Offshore wind
Tidal stream arrays
Hybrid
Cost of energy
Economics
Wake modelling

ABSTRACT

This paper evaluates the potential for co-location of offshore wind turbines at sites being developed for tidal stream arrays as a method for reducing the cost of electricity. It is shown that for a typical tidal site, MeyGen in the Pentland Firth, UK, increasing the wind turbine capacity reduces the cost of electricity compared to operating tidal stream arrays alone. This is due to increased energy yield combined with reduction of capital expenditure based on the use of common grid connection and shared support structures. Assessment is made using tidal, wave and wind resource data for a three year period. The overturning moment about the base of a monopile supporting a wind turbine with two tidal turbines is only 8% larger than for a wind turbine alone in a strong current typical of tidal farms. The increased cost of infrastructure is small relative to the increased energy yield and for all array configurations of practical interest, the levelised capital cost of energy is estimated to be 10–12% less from a co-located farm than from a tidal turbine farm alone.

1. Introduction

Offshore wind is rapidly becoming an established method of generating renewable energy, with installed capacity increasing by nearly 30% per annum and providing around 5% of total European Union (EU) renewable electricity generated in 2015 [1]. The United Kingdom provides 46% of EU offshore wind capacity, with the majority of this built in shallow water depths, typically less than 30 m. With plans to double capacity between 2015 and 2020 [2], much of this new deployment will be required to be built further from shore, in deeper water locations. Here, fixed-bed support structures become prohibitively expensive to build and offshore operations more time-consuming to execute [3].

Marine renewable energy (wave and tidal) are also emerging technologies with the potential for large scale deployment. In the UK, tidal stream energy has been estimated to have a potential of around 20 TWh/yr [4], with around 40 GWh/yr estimated for wave energy converters [5]. However, these technologies are at a pre-commercial stage, with high estimated costs of energy (targets for levelised-cost of energy are £ 150/MWh by 2020 for both wave [6] and tidal-stream [7]). Deploying multiple marine energy technologies at the same location (co-location) has been suggested as a method of reducing the economic cost from operating the technologies individually [8–10]. Co-location takes advantage of synergies, particularly shared electrical connections, foundations and smoothing of power output, which should reduce the cost of electricity generation. For example, a range of hybrid offshore wind and wave energy converters was considered as part of the European Union Seventh Framework Program (EU FP7) [11]. However, for systems with low ratios of wave to wind capacity (<20%), the additional cost and complexity of the wave energy converter (WEC) is typically too high to be considered of interest to device developers [8]. Hybrid devices are of most interest when the capacities are similar. Nevertheless, co-location of wave and wind devices on separate supports may still provide cost savings and smoothed power output [9,10]. Alternatively, co-location of wind and tidal stream turbines, with the higher annual available energy per unit area of the tides relative to the wind, has the potential to provide both a more even balance of capacity to warrant sharing support structures, as well as a smoother and less intermittent power supply. This method of co-location has received very little attention and is the focus of the present study, expanding on prior studies of array energy yield and loading [12–14].

This paper presents a holistic assessment of the economic benefits and challenges associated with deployment of wind turbines co-located within tidal stream farms. Alternative generating options are typically compared on the basis of the levelised cost of energy (LCOE). Here, the percentage change of capital cost and energy yield are assessed in order to evaluate the potential for reduction of LCOE relative to deployment of a tidal farm alone. Section 2 presents a range of baseline cost

* Corresponding author.
E-mail addresses: david.lande-sudall@hvl.no (D. Lande-Sudall), tim.stallard@manchester.ac.uk (T. Stallard).

https://doi.org/10.1016/j.rser.2019.01.035
Received 6 April 2018; Received in revised form 22 November 2018; Accepted 15 January 2019
Available online 07 February 2019
1364-0321/ © 2019 The Authors. Published by Elsevier Ltd. This is an open access article under the CC BY license (http://creativecommons.org/licenses/BY/4.0/).

Nomenclature

$\dot{U}_{wav}$	Wave-induced acceleration
C_D	Drag coefficient
C_m	Inertia coefficient
C_P	Power coefficient
D_T	Diameter of tidal turbine
D_W	Diameter of wind turbine
E_t	Energy yield in year, t
E_{comb}	Combined wind and tidal energy yield
E_{tidal}	Tidal energy yield
F	Total hydrodynamic force
I	Second moment of area
i	Row number
j	Turbine number on row, i
M	Overturning moment about base of monopile
r	Discount rate
T	Cost component for tidal-only turbine
U_0	Ambient flow velocity
U_c	Current velocity
U_{rate}	Rated speed of tidal turbine
$U_{shutdown}$	Shutdown speed of tidal turbine
$U_{w_{rate}}$	Rated speed of wind turbine
$U_{w_{shut}}$	Shutdown speed of wind turbine
U_{wav}	Wave-induced velocity
V	Volume of support structure
W_l	Cost component for a wind turbine-only in a low-current
x	Longitudinal distance
X_{space}	Longitudinal turbine spacing
y	Lateral distance
$y_{1/2}$	Half-wake width
ΔU	Velocity deficit
ΔU_{max}	Maximum velocity deficit
ϕ_{wav}	Wave heading relative to current heading
ρ	Density of sea-water, 1025 kg/m^3
σ	Monopile bending stress
σ_y	Yield stress
$LCOE$	Levelised-cost of energy
$LCOE_{CAPEX}$	Levelised-cost of energy based on capital expenditure
ACF	Array capacity factor
CAPEX	Capital expenditure
OPEX	Operational expenditure
T1	Tidal turbine-only support
T1W1	One tidal turbine on a single wind turbine monopile support
T2W1	Two tidal turbines on a single wind turbine central monopile support
W1	Separate wind monopile support

estimates for offshore wind and tidal stream farms separately. Energy yield for a range of co-located layouts, at a case-study site for MeyGen in the Inner Sound of the Pentland Firth, UK, is then considered in Section 3. The cost of the support structure is dependent on the peak loads experienced by the structure and so the results of modelling loads on different shared support concepts are presented in Section 4. Finally, combining the results of Sections 3 and 4, the capital cost and levelised cost of electricity for different co-located arrangements are evaluated in Section 5.

2. Baseline costs for offshore wind and tidal stream turbines

As a measure of comparing lifetime costs of alternative energy infrastructure projects, the levelised cost of energy (LCOE) is typically defined as [15–17]:

$$LCOE = \frac{\sum_t [(CAPEX_t + OPEX_t)(1+r)^{-t}]}{\sum_t [E_t(1+r)^{-t}]} \quad (1)$$

where $CAPEX_t$ is the capital cost associated with year, t, and includes the planning and development costs. $OPEX_t$ is the operational expenditure and E_t is the net energy generated in the t-th year with a discount rate, r reflecting the risk of the project.

OPEX can vary considerably with deployment location due to distance to port, vessel availability and the occurrence of weather windows suited for access [18]. For a given site, such costs will vary with the number of support structures and turbines installed. The comparison herein is focused on a farm of tidal turbines without and with a single wind turbine at a single location and so OPEX is not considered to simplify the analysis. Instead, the levelised cost of energy based on CAPEX alone ($LCOE_{CAPEX}$) is defined in Eq. (2), as introduced by [19]:

$$LCOE_{CAPEX} = \frac{\sum_{t=0}^{t=N} CAPEX_t(1+r)^{-t}}{\sum_{t=0}^{t=N} E_t(1+r)^{-t}} \quad (2)$$

There is considerable uncertainty in determining accurate whole life-cycle costs for new technologies. For offshore wind farms, where only the very earliest farms are reaching end-of-life and the technology is still maturing, the uncertainty is represented in the broad range of CAPEX and LCOE estimates given in a number of studies, such as [20–23]. Similarly, [24,25] provide estimated ranges on tidal stream CAPEX and LCOE, with future targets, post 2020 for second generation arrays, suggested by [7,26]. These CAPEX and LCOE estimates are summarised in Table 1 and provide baseline upper and lower bound cost estimates for this study. There is thus lower confidence in cost estimates for tidal stream arrays than for offshore wind farms, as these are based on a very limited number of prototype turbines, with little operational experience and sometimes with assumptions of technology and learning transferred from other industry sectors. Therefore, an estimate of the CAPEX can be made through consideration of how the main cost elements will differ for a co-located farm relative to farms of either wind or tidal stream turbines alone. As more accurate cost estimates become available, the cost analysis presented herein can be readily updated to reflect such changes.

Various other studies have addressed the percentage contribution of several cost centres to capital cost. For offshore wind farms this includes estimates by [27–30] and for tidal stream farms by [19,24,16,31]. From these studies, a representative breakdown of CAPEX costs per MW capacity for offshore wind and tidal stream have been derived and are presented in Fig. 1(a) and (b). This shows that between 22% and 27% of the CAPEX for offshore wind and tidal stream arrays is from the cost of the support structures (foundation and tower). Around 50% of this cost for offshore wind is from the cost of material and quantity of steel required to withstand the structural loads [30,32]. Accordingly, the maximum loads acting on a shared support structure are assessed in Section 4 for various combinations of metocean conditions and turbine operating states. Prior to this, Section 3 examines the energy yield for a

Table 1
Upper and lower-bound CAPEX and LCOE estimates for offshore wind and tidal stream projects. Offshore wind CAPEX and LCOE ranges are derived from [22,23]. Tidal stream CAPEX range is defined from a combination of commercial scale array prices of [25] and 2020 targets for large arrays from [7]. Tidal LCOE estimates are from [7] 2020 targets and [26] second generation arrays.

	CAPEX, £ m/MW	LCOE, £/MWh
Offshore wind	1.5–3.5	100–140
Tidal stream	2.25–4.0	150–320

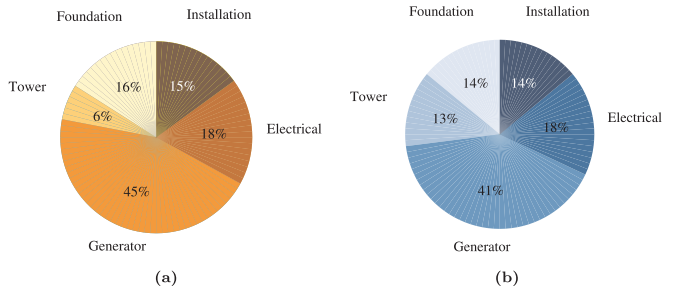

Fig. 1. Indicative cost breakdown per MW capacity for (a) offshore wind and (b) tidal stream.

co-located farm, since the $LCOE_{CAPEX}$ is shown in Eq. (2) to be dependent on energy yield generated over the life of the project.

3. Energy yield for a co-located farm with shared supports

In an earlier study by the authors [14], energy yield for a farm of 12 MW wind capacity co-located with a 20 MW rectilinear tidal array was considered at a case-study site of MeyGen in the Inner Sound of the Pentland Firth, UK [33]. As for wind turbines, it is important to account for the wake interactions of tidal stream turbines since downstream turbines are shielded to some degree and these are modelled using a method of linear superposition of self-similar wakes [34]. That approach is modified here to account for differing wakes of tidal stream turbines with a larger support structure in order to more accurately estimate the energy yield from a co-located farm. The array capacity factor (ACF) is defined as the ratio of electricity generated to that which would be generated if the array operated at full capacity over the same period of time. It therefore gives a measure of utilisation of the installed capacity. A range of array capacity factors are considered against an extended set of resource data so that the effect of array layout on energy yield, and hence costs, can be assessed.

3.1. Idealised wind: tidal capacity ratio

The ratio of installed capacity of wind turbines to installed capacity of tidal stream turbines is referred to as the 'wind:tidal capacity ratio'. In [14], this was 0.6, however the intra-array tidal turbine spacing was large, with 20 tidal rotor diameters (D_T = 20 m) in the longitudinal and $5D_T$ in the lateral directions. The four additional 3 MW wind turbines provided an extra 80% energy yield compared to operating the tidal array alone. A site developer may consider closer tidal turbine spacing, such as $10D_T$ longitudinal, with cross-stream spacing of $1.5D_T$ having been studied by [35] and even $1.1D_T$ by [36]. With more tidal turbines and the same wind turbine capacity, the installed array capacity ratio would be less than 0.6. To establish a worst case scenario in terms of increasing energy yield by co-locating wind turbines, the minimum increase in energy yield, $(E_{comb} - E_{tidal})/E_{tidal}$, is assessed for a ratio of wind:tidal capacity smaller than 0.6 by increasing the number of tidal turbines thus reducing their spacing to a practical minimum (assuming no bathymetric or other 'external' restrictions on turbine placement). To facilitate comparison between alternative tidal turbine array configurations a 'unit' within a co-located array is considered, defined by the plan area around a single 3 MW wind turbine within a wind farm, defined here as 11 wind rotor diameters, D_W, longitudinally and 3.5 D_W laterally, in order to compare with [14] (note $D_W \sim 5.5D_T$). This means that only one wind turbine is considered per unit array-area and so wind turbine wake effects are neglected. This approach also means that the tidal arrays modelled are between two and six rows and so the superposition method is not applied significantly beyond the demonstrated range of validity for this method of three-to-four row arrays.

3.2. Array energy yield including support structure wakes

The model in [14] neglected the wake due to support structures. For arrays of tidal stream turbines only, where the diameter of the support is around $0.1D_T$ [37,38], this is an adequate assumption, since the wake due to a support of this scale has decayed by around 1 to $2D_T$ downstream [39,40]. This rotor-only far-wake is described by a depth-averaged plane wake with a self-similar Gaussian profile, Eq. (3), from approximately $6D_T$ downstream.

$$\Delta U(x, y) = \Delta U_{max} \exp\left(-ln(2)\frac{y^2}{y_{1/2}^2}\right) \tag{3}$$

Where the velocity deficit, $\Delta U = U_0 - U$. The recovery of centreline deficit, ΔU_{max} with streamwise distance, x, is given by Eq. (4) where $k_U = 1.0512$ and $k_{0U} = -0.1579$ and half-wake width, $y_{1/2}$, as Eq. (5) with $k_W = 0.4243$ and $k_{0W} = 0.2159$.

$$\frac{\Delta U_{max}}{U_0} = k_U (x/D)^{-1/2} + k_{0U} \tag{4}$$

$$\frac{y_{1/2}}{R} = k_W (x/D)^{1/2} + k_{0W} \tag{5}$$

These equations can be used in a method of linear superposition of velocity deficits to represent the wake of multiple devices to a good degree of accuracy [34]. The deficit behind the i-th row of turbines, ΔU_i at distance x_i downstream, is due to the superposition of all upstream turbine wake deficits (Eq. (6)). In other words, the deficit from the first row of turbines provides the onset flow profile to the second row, with the deficit of the second row providing the onset flow for the third row and so on.

$$\Delta U_i(x_i, y_i) = \Delta U_{i-1}(x_i, y_i) + \sum_{j=1}^{n} \Delta U_j(x_i, y_i) \;\; ; x_i \geq 6D_t \tag{6}$$

Where n is the number of turbines on the ith-row and x_i is the perpendicular downstream distance (aligned with bulk flow direction) from row i; y_i is orthogonal to x_i.

However, in the case of co-location, the support diameter of the wind turbines, or shared supports for combined wind and tidal stream turbines, will be much larger, possibly as great as 0.25 D_T (0.045 D_W) [41]. This study uses the findings of [42] to represent the wakes due to different support structures, where the far-wake velocity deficit of the supports are also described by the self-similar Gaussian profile of Eq. (3). Alternative support structure configurations (Fig. 2) are considered for each co-located array layout with one wind turbine:

- 'W1' – separate wind monopile.

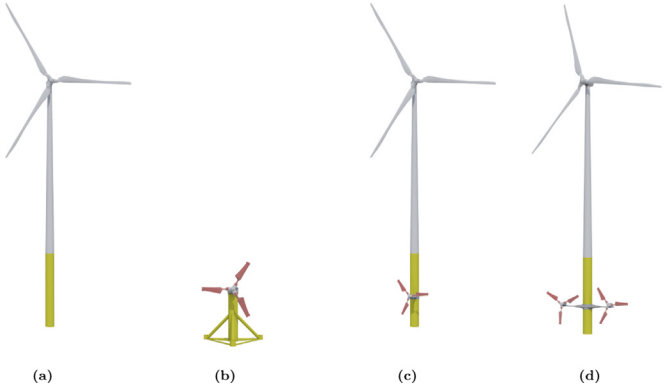

Fig. 2. Support structure types considered: (a) wind-only monopile ('W1'), (b) tidal turbine-only ('T1'), (c) one tidal turbine on a single wind turbine monopile ('T1W1') and (d) two tidal turbines on a single wind turbine monopile support ('T2W1').

- 'T1' – tidal turbine-only (negligible tower wake).
- 'T1W1' – one tidal turbine on a single wind turbine monopile.
- 'T2W1' – two tidal turbines on a single wind turbine central monopile support.

Wake parameters from Eqs. (4) and (5) are shown for each support type in Table 2, with the T1W1 support obtained as the superposition of the T1 and W1 wakes. The velocity deficit field for each array layout is then established for a range of inflow headings, as in [14]. This is used as a look-up table against the time-series current resource data to calculate the resulting power output for the array of 1 MW rated tidal turbines with power curve defined as in Fig. 3 and a slack-tide yaw mechanism implemented as in [14]. Energy yield from the 3 MW wind turbine is calculated based on a power curve for a 100 m diameter rotor, achieving rated power at 12 m/s and with a shutdown speed of 25 m/s, (see Fig. 3) as described in [14].

3.3. Resource data

For commercial viability of tidal stream arrays, it has been suggested that current velocities greater than 2 m/s are required [43]. Global sites of interest for commercial deployment of tidal stream arrays typically have peak spring velocities exceeding 3 m/s [44–46]. The Pentland Firth, UK is suggested to carry the majority of the UK's potentially extractable tidal current resource [47]. With peak spring tides measured by a number of Acoustic-Doppler Current Profiler (ADCP) measurement campaigns exceeding 4 m/s [48,49], and a lease for 800 MW tidal stream capacity, the Inner Sound of the Pentland Firth is of significant interest for tidal stream development. These ADCP measurements have been used to validate a number of numerical ocean circulation models at varying degrees of resolution [50–52]. The models demonstrate a directional asymmetry between the flood and ebb tides [48], and this led to turbines with a slack-tide yaw strategy being implemented in [13] to maximise tidal energy yield compared to using fixed turbines. The low-lying land around the Inner Sound was also suggested to give a reasonable wind climate for wind generation, with annual Weibull distribution scale and shape parameters of 8.3 and 2.0 m/s respectively [14].

This study focuses on a time-series analysis of coincident tidal stream velocity and heading, wind velocity and heading, and wave statistics. Several sources of data are considered, as follows. Three years of wind resource data from the 1.5 km spatial resolution UK Met Office UKV model [53] has been scaled using a method of measure-correlate-predict (MCP), to 8 weeks of 400 m resolution Weather Research and Forecasting (WRF) data run for the site, as described in [14] and shown in Fig. 3(b). Similarly, a 2-dimensional ADvanced CIRCulation (ADCIRC) oceanographic model, with six months of data at 150 m resolution, was used to correct tidal current velocity data, provided by the E.U. Copernicus Marine Environment Monitoring Service, from a 7.5 km Forecasting Ocean Assimilation Model (FOAM) [54] also using a MCP method. This resource data (Fig. 3(c)) is used as input to the energy yield model (and loads model in Section 4) and is described in further detail in [14]. Coincident wave parameters from the ERA-Interim dataset [55] have been correlated in the same manner with six months of wave buoy data (Fig. 3(d)–(e)).

3.4. Energy yield results

3.4.1. Energy yield for aligned and staggered array layouts

In order to identify the maximum energy yield from a unit area within a co-located array, the number of rows of tidal turbines is stepwise increased from 1 to 6 rows of 13 turbines per row with cross-stream spacing of 1.5 D_T. For all layouts, downstream spacing is specified as uniform between all rows within the 60 D_t unit area length boundary. It is assumed that the superposition model will be accurate for up to six rows of turbines. Energy yield for all layouts using the T2W1 device is given in Table 3 and presented against capacity-area density in Fig. 4, where capacity-area density is defined as the ratio of installed capacity per unit area.

Four rows of 13 turbines (4row13) is found to give the maximum tidal energy yield. Each additional row of turbines acts to reduce the net yield with the array capacity factor for the 6row13 layout being almost half of that for the 4row13 array despite it having greater installed capacity. Comparing the wake velocity deficit fields of Fig. 5(a) and (b), it can be seen that the deficit entering row 3 of the 6row13 layout is very high, suggesting a low capacity factor for turbines on rows three and four (when flow is from left-to-right). However, it can be seen from $E_{comb}/E_{tidal} - 1$ in Table 3 for the 4row13 layout that the wind turbine only gives an extra 12% energy yield compared to that generated by the tidal turbines alone. This is far less than the 28% additional energy the wind turbine provides to the 1row13 layout.

For the same density and spacing, the influence of wakes on downstream turbines can be reduced if the turbine positions are staggered, giving higher energy yield. Table 3 compares both aligned and staggered turbine layouts. For the 4row13 case, the increase in tidal energy yield by moving to a staggered array is less than 1% and so the ratio of combined to tidal energy yield, $E_{comb}/E_{tidal} - 1$ is still around 12%. Since the difference is small, only aligned layouts are considered in the remaining analysis.

For multiple unit array-areas with several interacting wind turbines, wind turbine wakes would need to be considered. In [14], it was suggested that wind farm wake losses were around 7%, such that if this level of loss is included in the single unit array-area analysis, the ratio of combined-to-tidal energy yield reduces to approximately 11.5%.

3.4.2. Comparison of energy yield for co-located devices

The wake due to the T2W1 support was shown in [42] to recover at a slower rate than both the wake of a single turbine and the wake of the T1W1 co-located device. This is seen in Fig. 5(b) where the T2W1 wake propagates through the whole array, whilst the wake of the T1W1 device (Fig. 6(a)) is barely distinguishable from the individual tidal turbine wakes. [42] also showed that the power coefficient, C_P, from each tidal turbine during rated operation in the T2W1 configuration increased by 25% due to increased blockage compared to rotor-only operation, whilst the power from the tidal turbine of the T1W1 device reduced by approximately 25%. The rotors in both configurations were not designed for such operation and an optimally designed rotor may generate more power [56]. To assess the impact of these potential changes of rotor performance on array energy yield, the model has been run for the T1W1 device both with and without a 25% reduction in C_P, whilst the T2W1 has been run both with and without a 25% increase in C_P. The results are shown for both the 2row13 and 4row13 array layouts in Table 4.

Even with a 75% reduction in C_P, the arrays with T1W1 devices generate slightly more energy yield than for all layouts with the T2W1 device and 25% increase in C_P. The configuration with separate wind turbines (W1) generates least energy yield in the 4row13 layout but generates more than the T2W1 device type in the 2row13 layout, where longitudinal spacing between turbine rows is large enough that the wake of the wind turbine support is recovered to 95% of the free-stream velocity when incident to the downstream turbines. The device arrangement generating maximum energy yield is hence dependent on

Table 2
Wake parameters for alternative support structure configurations of Eqs. (4) and (5). Wake for T1W1 is obtained as the linear of superposition of T1 and W1.

Support type	k_U	k_{0U}	k_W	k_{0W}
T1	1.0512	− 0.1579	0.4243	0.2159
W1	0.2937	− 0.0017	0.2899	0.0701
T2W1	0.9069	0.0431	− 0.2450	2.8211

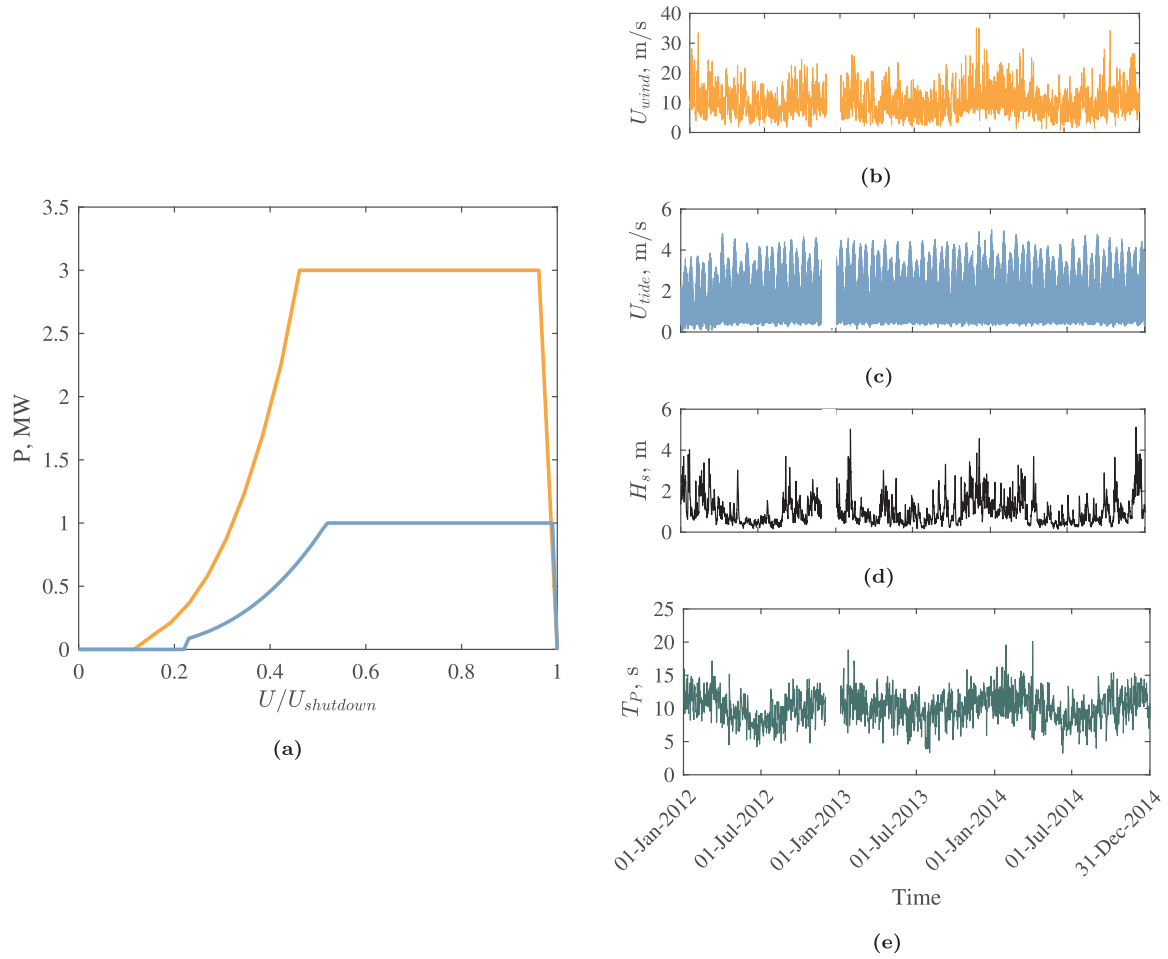

Fig. 3. (a) Power curves for the wind (orange) and tidal (blue) turbines. Shutdown speed is defined as 25 m/s for the wind turbine and 5 m/s for the tidal turbine. Time series of input (b) hub-height wind speed, (c) undisturbed tidal current speed, (d) 3-hour significant wave height, H_s and (e) corresponding peak wave period, T_P, for the period 01 Jan 2012–31 Dec 2014 (excl. Dec 2012 due to lack of availability).

Table 3
Comparison of energy yield and array capacity factor (ACF) for the period 01 Jan 2012–31 Dec 2014 (excl. Dec 2012 due to lack of availability) for aligned and staggered tidal array layouts with 13–78 MW capacity, featuring a T2W1 shared support structure located on the front row. Downstream tidal turbine spacing is specified as uniform between all rows within the 60 D_t length boundary and cross-stream spacing is fixed at $1.5D_T$. Wind energy yield is 42.72 GWh for all layouts.

Layout	Longitudinally	X_{space}, D_T	Tidal		Combined		$E_{comb.}/E_{tidal} - 1$, %
	Aligned/Staggered		GWh	ACF	GWh	ACF	
1row13 (13 MW)	–	60	151.28	0.455	194.00	0.474	28.2
2row13 (26 MW)	Aligned	30	274.52	0.413	317.19	0.428	15.6
	Staggered		274.47	0.413	317.19	0.428	15.6
3row13 (39 MW)	Aligned	20	341.11	0.342	383.82	0.358	12.5
	Staggered		342.16	0.343	384.88	0.359	12.5
4row13 (52 MW)	Aligned	15	355.81	0.268	398.52	0.284	12.0
	Staggered		358.48	0.270	401.20	0.285	11.9
5row13 (65 MW)	Aligned	12	322.85	0.194	365.57	0.210	13.2
	Staggered		340.99	0.205	383.71	0.221	12.5
6row13 (78 MW)	Aligned	10	301.12	0.151	343.84	0.166	14.2
	Staggered		313.3	0.157	356.02	0.172	13.6

the array layout. However, given that the differences in yield between each device configuration are small (~ 2%), each device will need to be assessed individually to see which can deliver the largest cost of electricity reduction. To be conservative, and since it is not clear how power output would vary for an optimally designed rotor, devices are herein considered with power output unchanged (i.e. C_P is not increased for the T2W1 device, etc.).

4. Shared support structural loads

Around 50% of the cost of wind turbine foundations is from the material cost [30,32]. Various models exist for estimating the cost of

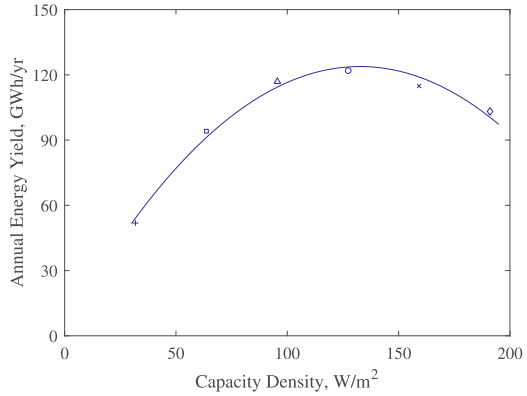

Fig. 4. Average tidal array energy yield per year (GWh/yr) versus capacity area density (W/m^2) for the aligned array layouts with 1–6 rows of tidal turbines (markers order: +, □, △, ○, ×, ◇) with 13 turbines per row along with corresponding least-squares fit quadratic curves. Contribution from wind turbine is neglected.

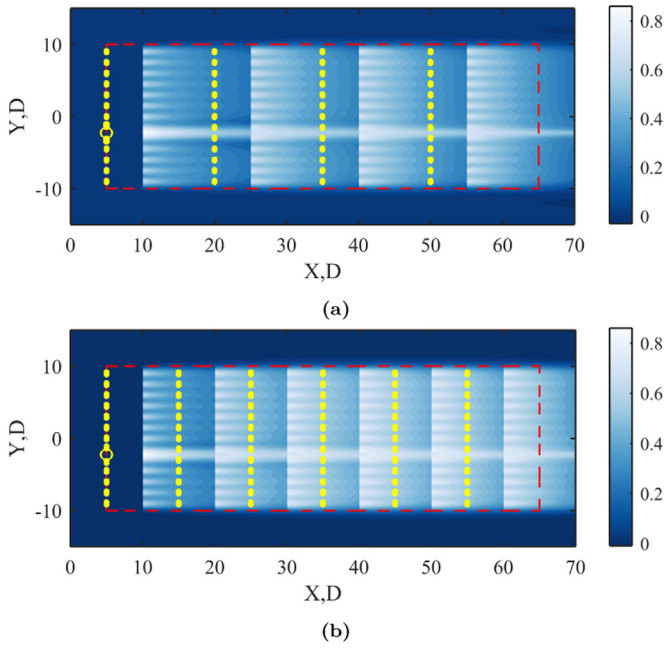

Fig. 5. Velocity deficits for (a) 4row13 and (b) 6row13 aligned array layouts with normal in-flow heading. Yellow markers represent positions of tidal-only devices (•) and the T2W1 shared device (◉). Wake superposition started at 5 D_T behind each rotor plane. Unit-area boundary (red-dashed line).

steel monopile foundations [57,58], and typically these are proportional to the overturning moment applied and the water depth in which the turbine is located. The mass of steel used is also proportional to the water depth [59] and so the cost of foundation is taken to be directly proportional to the mass of steel used. However, offshore wind turbines with the capital cost breakdown of Fig. 1 are typically located in regions of low current speed, U < 2 m/s is typical for the North Sea [60,61]. To determine the mass of steel required for a co-located support structure subject to flows of up to 4 m/s at the deployment site, monopile wall thickness is obtained based on peak overturning moment using the approach detailed in [14]. This method accounts for the operating states of the wind and tidal stream turbines across the range of wind, wave and current conditions occurring at the site.

A monopile foundation is considered, with nominal diameter 5 m. Wind turbine thrust is obtained using the thrust curve from a 3 MW Vestas V90 turbine [62] and thrust for the tidal turbine(s) using the thrust curve for a full-scale fixed-pitch device as in [14]. Environmental

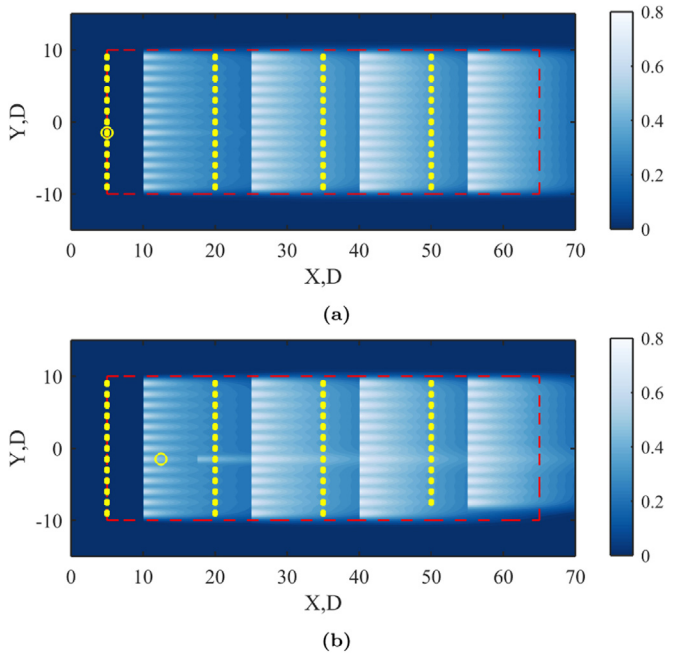

Fig. 6. Velocity deficits for 4row13 array layout with (a) T1W1 shared support (◉) and (b) W1 - separate wind (◯) and tidal supports (•). Wake superposition started at 5 D_T behind each rotor plane. Unit-area boundary (red-dashed line).

Table 4
Tidal energy yield (GWh) and array capacity factor (ACF) for the period 01 Jan 2012–31 Dec 2014 (excl. Dec 2012) for arrays of 2 row 13 and 4 rows 13, 1 MW tidal stream turbines with 1.5 D_t lateral spacing and 30 D_t and 15 D_t longitudinal spacing, respectively. Shared support configurations of T2W1 and T1W1 are compared to separate wind and tidal supports (W1). Combined energy yield can be obtained by addition of wind energy yield, which is 42.72 GWh for all layouts.

Support type	2row13		4row13	
	GWh	ACF	GWh	ACF
W1	276.27	0.416	352.06	0.265
T1W1	278.54	0.419	364.59	0.274
T1W1 (0.75C_P)	276.93	0.417	362.98	0.273
T2W1	274.52	0.413	355.81	0.268
T2W1 (1.25C_P)	276.83	0.417	358.12	0.269

conditions are input using the time-series data from the energy yield model of Section 3, with turbulent wind and current specified using the Normal Turbulence Model definitions of [63]. Wave kinematics for a single wave form, representative of a wave with 1% occurrence statistics, are obtained using a non-linear wave model based on [64]. Hydrodynamic loads, aligned with the current direction, are then obtained as the modified Morison equation [65]:

$$F = \frac{1}{2} C_D \rho A |U_c + U_{wav} \cos\phi_{wav}| (U_c + U_{wav} \cos\phi_{wav}) + \rho V C_m \dot{U}_{wav} \quad (7)$$

where ϕ_{wav} is the angle between wave and current headings, coefficient of inertia, $C_m = 2$ and coefficient of drag is dependent on the Keulegan-Carpenter number, as in [66]. A modification to the wave force to account for breaking follows the method in [67]. Wave loads on the tidal turbine rotors are obtained separately, following the method of [68]. Full details of this load model are given in [14].

Four structural configurations are modelled:

- Wind turbine-only in current <2 m/s (W1 low-current);
- Wind turbine-only in strong tidal current (W1 high-current);
- T1W1 device in strong current;

- T2W1 device in strong current.

For the W1 low-current device, the peak force is calculated using the same time-series force calculation described above, but with the current speeds linearly scaled so that the peak current speed is never greater than 2 m/s. For the T2W1 device, [42] showed the load on the central tower due to increased blockage was 9.05% greater than the tower-only drag. The drag coefficients used for the tower in the T2W1 load model are increased by 9.05% to account for this increased load.

4.1. Support structure loads

The time history of the magnitude of peak overturning moment for the T2W1 arrangement is compared to that predicted for the T1W1 in Fig. 7. Each of the highlighted peak load cases are detailed in Table 5.

The mean overturning moment on the T2W1 device is 16.8% greater than that for the T1W1 case. The maximum load for the T2W1 occurs in the rated-shutdown condition as opposed to the wave shut-down-shutdown condition for the T1W1 device. However, the difference between the magnitudes of these maximum loads is only 4.4% greater for the T2W1 structure. This latter result shows that an additional tidal turbine only requires the structure to be designed with an extra 4.4% overturning moment capacity than for the T1W1. Note, the difference between peak overturning moment values for the T1W1 device in Table 5 and those reported in [14] is approximately 18%. This difference is purely due to using a monopile foundation here, which experiences a greater drag force than the tripod foundation used in [14].

A summary of the mean and peak loads for each structure configuration are given in Table 6. The peak load for the T1W1 structure is less than 1% greater than the W1 in high current. This is because the shutdown tidal turbine adds very little extra drag. Similarly, the T2W1 structure is only 4.5% greater than for the W1 device in high current, suggesting that two turbines can be added to the support with very little increase in base overturning moment. However the load on the W1 structure in high current is 54% greater than in low current. The following section assesses whether a structure could be designed to withstand such an increased load, whilst maintaining the same monopile diameter, by increasing the wall thickness only.

4.2. Design load failure analysis

Following the Ultimate Limit State design of DNV [63], a minimum wall thickness can be determined for each structure which satisfies the following relation:

$$\sigma \leq \frac{1}{\gamma_f}\frac{1}{\gamma_m}\frac{1}{\gamma_n}\sigma_y \tag{8}$$

where partial safety factors for load, material and consequence of failure are defined as $\gamma_f = 1.35$, $\gamma_m = 1.1$ and $\gamma_n = 1$ respectively, σ_y is the yield stress of mild steel (250 MPa) and σ is the maximum bending stress in the monopile, found as the Euler-Bernoulli bending load equation:

$$\sigma = \frac{Mz}{I} \tag{9}$$

In Eq. (9), bending moment is M, second moment of area for a circular cylinder, I and distance from neutral axis to material surface, z. Using the loads from Table 6, the minimum wall-thickness is calculated as 82 mm for the W1 low-current case. In contrast, the thickness calculated for the W1 high-current device was around 60% greater (129 mm). Minimum wall thickness for the T1W1 is the same (to the nearest 1 mm), whilst that for T2W1 device is 135 mm. Such wall thicknesses are large, but compare to the maximum used in offshore wind turbine monopiles of 150 mm [69] and so are possible to fabricate. However, an actual combined support structure may well need to be designed differently in order to satisfy other load requirements, such as for fatigue which will likely be high due to the increased unsteady loads for the T2W1 structure [42]. However, such considerations are beyond the scope of this study. For a column foundation with height extending 5 m above the mean water level (35 m), the foundation cost will increase by the corresponding increase in mass due to this wall thickness compared to the typical structure for a wind turbine only at a low-current site. These results are used in the following section for analysing potential cost savings by installing co-located devices compared to either technology alone.

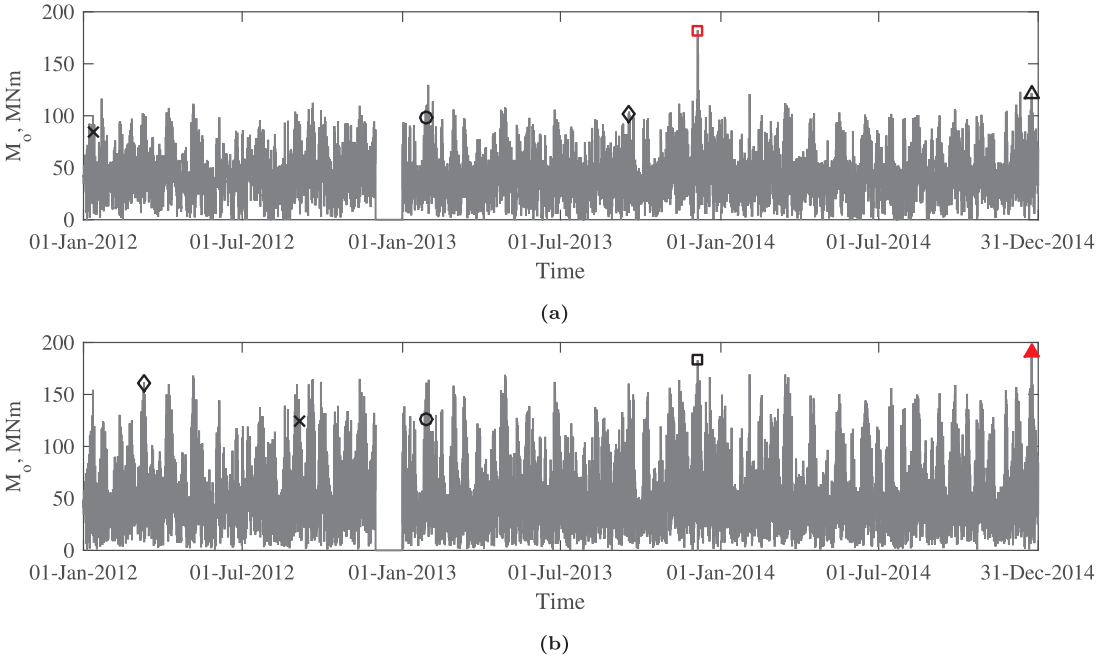

Fig. 7. Base overturning moment magnitude for (a) combined wind turbine with single tidal turbine on monopile foundation (T1W1) and (b) combined wind turbine with 2 tidal turbines side-by-side of a monopile foundation (T2W1); for the 3 year period (excluding December 2012) of coherent wind, wave and current data. The five load scenarios as defined in Table 5 are identified in order as ○, △, ×,◇, □ with maximum overturning moment for each system highlighted in red.

Table 5
Overturning moment magnitudes for the combined structure with 1 tidal turbine (1T1W) and 2 tidal turbines (2T1W) during operation at near-to -rated and -shutdown speeds* for each the wind and tidal turbine(s) located at location 1. Maximum load is highlighted in bold.

Wind Turbine: Tidal Turbine(s):	Rated[1] Rated[3]	Rated[1] near-Shutdown[4]	near-Shutdown[2] Rated[3]	near-Shutdown[2] near-Shutdown[4]	Shutdown Shutdown[+]
1 rotor-tower, MNm	98.33	121.70	84.12	102.30	**182.36**
2 rotor-tower, MNm	162.23	**190.30**	124.07	161.53	182.93

*Wind turbine: [1] Rated = $11 < U_{wrate} < 20$ m/s; [2] near − Shutdown = $20 \leq U_{wshut} < 25$ m/s.
Tidal turbine: [3] Rated = $2.3 < U_{rate} < 3$ m/s; [4] near − Shutdown = $3 \leq U_{shutdown} < 5$ m/s.
For these four cases, $H_s < 3$ m was considered. [+]The final shutdown-shutdown case is the extreme case of all turbines parked in shutdown and with $H_s > 3$ m.

Table 6
Summary of maximum and mean overturning moment magnitudes obtained from the three-year time-history of loads for the W1 structure in low- and high-current, and for shared supports of 1T1W and 2T1W.

Support type	Maximum (MNm)	Mean (MNm)
W1 low-current	118.5	37.1
W1 high-current	182.2	39.3
1T1W	182.4	39.8
2T1W	190.3	46.5

5. Cost analysis of co-located farms

Many of the component costs for a co-located platform can be inferred from costs for offshore wind and tidal stream turbines. These were reviewed in Section 2. However, in order for an offshore wind turbine to be erected in a high current location, the costs of the foundation, installation, and electrical infrastructure will all be affected, and these are considered below.

5.1. Capital cost centres

5.1.1. Cost of support structure

The cost of the support structure consists of the foundation (structure below transition piece) and tower (above and including transition piece). The cost of foundation has already been considered to be proportional to the increase in steel mass used in the foundation. Since the same wind turbine tower can be used for all co-located devices, the CAPEX associated with the tower is the same for all devices.

5.1.2. Costs of electrical infrastructure

The majority of the costs of electrical infrastructure for offshore wind farms are due to the offshore substation (48%) and cabling (34%) [30]. Due to the proximity of the case-study site to shore, an electrical substation will not be required. The cost of the export cable to shore, which for an offshore wind turbine is around 80% of the cabling cost [30], is a function of the overall farm capacity as opposed to device number. In other words, many smaller capacity devices or few larger capacity devices could connect to the same export cable. It can be expected that this electrical cost breakdown is also similar to tidal stream arrays. The only real differences in the electrical costs per MW for offshore wind and tidal stream will be due to the inter-array cable costs (three, 1 MW tidal devices are required to be connected for each 3 MW wind turbine) and the environment for which the infrastructure is designed. It is hence estimated that the per MW cost for a co-located device will be the same as for a tidal-only array, minus the cost of two inter-array connections.

5.1.3. Cost of installation

Overall installation cost can be broken down into costs associated with installation of foundation, cables, and turbine deployment. Each of these categories represents approximately a third of the overall installation cost for standard offshore wind turbines [30] and a similar percentage breakdown is assumed for tidal stream turbines. Overall installation cost is largely dependent on vessel charter costs, availability, weather windows and site accessibility [70,71]. Early demonstration tidal turbines have used jack-up barges, such as used for offshore wind [72] and so vessel charter costs may be assumed comparable. Alongside wind speed and significant wave height limiting marine operations for offshore wind installation, weather windows for tidal turbines will additionally be limited by the high current speeds [71]. However modified jack-up barges have been used in 3.2 m/s current [72] and specialist vessels capable of operating in greater currents are becoming available [73,74]. As such, suitable weather windows for installation at a strong tidal site may not be any less frequent than for an offshore wind site. This could be assessed further, such as using the probability-based approach in [75], however is beyond the scope of this work. Once the foundation is in place, the speed and cost of device deployment, is dependent on the number of offshore lift operations required. For offshore wind turbines, with various assembly methods [76], four lifts is typical [77]. This compares with a single lift or towing operation used to deploy existing prototype tidal turbines [78,79]. Without further evidence, the cost of installing a wind turbine in a strong tidal current, is assumed the same as installing a single tidal stream device plus the cost due to an additional three offshore lifts. Here, the cost of each lift operation is calculated assuming the fraction of the installation cost for tidal turbine deployment is the same as the cost of a single lift (i.e. the cost of each additional lift is equal to a third of the overall installation cost for a single tidal turbine). The sensitivity of this assumption is evaluated in Section 5.1.4 and can easily be adjusted in future analyses to include more detailed information.

Table 7
Summary of cost assumptions for W1 - low current, T1, W1 - high current, and shared structures of T1W1 and T2W1. Each cost component is either from tidal-only (T), wind-only in low-current (W_l) or a stated combination of the two. The total number of offshore lifts, n is assumed 4 here, and '*cables*' refers to inter-array cable cost. The sum of all components gives the CAPEX for each structure type.

	Tower	Foundation	Installation	Electrical	Generator	CAPEX
W1 – low current	W_l	W_l	W_l	W_l	W_l	$CAPEX_{W_l}$
T1	T	T	T	T	T	$CAPEX_{T}$
W1 – high current	W_l	$W_l \times (W_h/W_l)_{mass}$	T	$T - 2W_l(cables)$	W_l	$CAPEX_{W_h}$
T1W1	W_l	$W_l \times (T1W1/W_l)_{mass}$	$T + (n-1)T/3$	$T - 2W_l(cables)$	$1\,T + W_l$	$CAPEX_{T1W1}$
T2W1	W_l	$W_l \times (T2W1/W_l)_{mass}$	$T + (n-1)T/3$	$T - 2W_l(cables)$	$2\,T + W_l$	$CAPEX_{T2W1}$

5.1.4. Aggregated capital costs

The assumptions made for the CAPEX per structure type are summarised in Table 7. Applying these assumptions gives the new CAPEXs associated with installing a wind turbine in a strong tidal current in Fig. 8(a) and shared devices to support one wind turbine with either one tidal turbine (T1W1) or two tidal turbines (T2W1) in Fig. 8(b) and (c) respectively. Based on the upper and lower CAPEX estimates from Table 1, the CAPEX range for the wind turbine in a strong current is determined as £1.8–3.8 m/MW and for the shared support structures ($CAPEX_{T1W1}$ and $CAPEX_{T2W1}$) as £1.6–3.3 m/MW and £1.5–3.1 m/MW, respectively. These ranges are represented by the extent of the bars in Fig. 9 and have upper bounds less than the upper bound costs for tidal-only arrays.

Each of the assumptions made above has an uncertainty. To test the sensitivity to each assumption, each of the cost categories with the upper-estimate are adjusted by ± 50%. In the case of the foundation and installation costs, it was assumed these could not be less than those for a wind-only device (in a strong tidal current). The error bars show that greatest sensitivity to CAPEX is from costs associated with the electrical infrastructure and installation. In all cases, the maximum CAPEX never exceeds the upper CAPEX estimate for a tidal turbine-only and so cost savings compared to a tidal-only array should be realisable.

5.2. Cost of energy for co-location compared to tidal only

Using the CAPEX ranges from Fig. 9, the $LCOE_{CAPEX}$ is calculated as Eq. (2) for each array layout. The lifetime of the project, N is defined as 20 years and the energy generated in each year, E_t is considered equal to the average energy per year from Section 3.4.1. An equal discount rate, $r = 0.1$ is applied to wind-only, tidal-only and combined systems, since these are typical values used in offshore wind [15] and tidal stream [19] and a combined system is expected to not present significantly greater risk than that for a tidal stream array. The results are presented against capacity-area density in Fig. 10.

For both the mean and upper CAPEX estimates, co-location (green) reduces the $LCOE_{CAPEX}$ compared to tidal-only (blue) by approximately 10% for all capacity-area densities. This increases to approximately 16% for the high capacity-area densities (5rows13) when total installed capacity of the co-located farm is kept the same as the tidal-only array. For the lower CAPEX estimates, $LCOE_{CAPEX}$ for the co-located array is 13% lower for low capacity densities and 17% lower at high capacity densities.

The triangle markers in Fig. 10, show the $LCOE_{CAPEX}$ for a 3 MW wind-only (low current) device, 3 MW tidal-only array and a 6 MW co-located farm featuring a single 5 MW combined device and an additional 1 MW tidal turbine arranged with the same tidal array footprint as the 3 MW tidal-only array. The respective $LCOE_{CAPEX}$ of these wind-only and co-located arrangements are 65% and 73% of the tidal-only cost.

The $LCOE_{CAPEX}$ for using T1W1 shared supports and separate wind and tidal support structures was also calculated for each of the array layouts (dashed and dotted lines respectively in Fig. 10). For separate

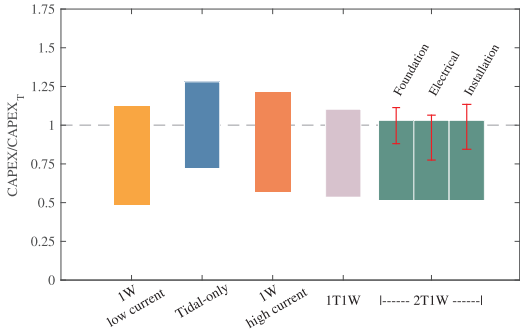

Fig. 9. CAPEX ranges normalised by central tidal CAPEX estimate, $CAPEX_T$, for: W1 low-current ( ), W1 high-current ( ), T1 ( ), T1W1 ( ) and T2W1 ( ). Upper and lower-bounds for W1 high current and combined systems are with inputs of upper and lower bound CAPEX estimates from Table 1, respectively. Red error bars show sensitivity of T2W1 to ± 50% changes in each cost parameter.

wind and tidal supports this was found to be close to the T2W1 shared support. The T1W1 device has a marginally lower cost at higher capacity-area densities and slightly higher cost at low capacity-area densities. Coupled with modelling errors and cost uncertainties, it is not possible to establish beyond doubt whether a shared or separate support structure offers a cheaper method of co-location.

Although the lowest $LCOE_{CAPEX}$ occurs for low density farms, maximum energy yield is shown by Fig. 4 to be at higher capacity-area densities of between 100 and 150 W/m^2. With the number and net area of potential tidal sites geographically limited, it is likely that exploitation of energy from each site will need to be prioritised. Following the targets in [7], an $LCOE_{CAPEX}$ of £80/MWh is henceforth considered as a benchmark for becoming commercially competitive. Given that normalisation in Fig. 10 was with $LCOE_{CAPEX_T}$ = £88/MWh, a tidal-only array only becomes cost competitive by using the minimum tidal CAPEX estimate and with arrays of up to ~ 64 W/m^2 capacity-area density. In contrast, if the lower CAPEX estimate is realised for co-location, an $LCOE_{CAPEX}$ less than £80/MWh is achievable with capacity-area density ~ 100 W/m^2. This is close to optimum capacity density for the array area. In other words, for the same area, a co-located farm could be built which generates over 20% extra energy yield than a tidal-only array with equivalent $LCOE_{CAPEX}$.

5.3. Varying wind turbine capacity

Sensitivity to changing the wind turbine capacity has also been studied for the 1row13 and 4row13 array layouts (Table 8) with results plotted in Fig. 10. For this analysis, the wind turbine capacity was varied between 0 and 6 MW by simply scaling the 3 MW wind turbine's rotor diameter to achieve the desired turbine rating. Peak power coefficient, $C_{P_{max}}$ was assumed to stay the same and cut-in and shutdown speeds were kept constant. This is identical to scaling the 3 MW wind turbine's power curve (Fig. 3) by a given factor, α_s, to achieve the same

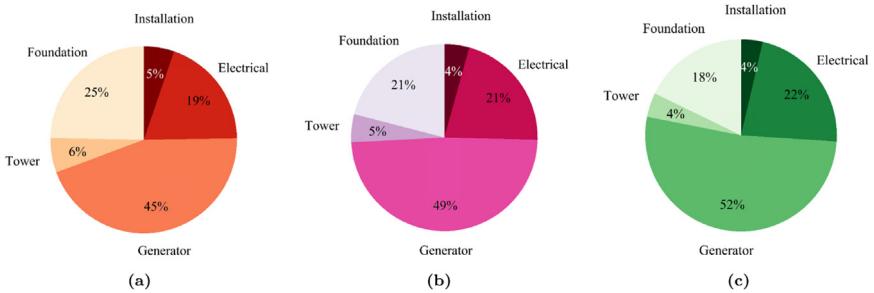

Fig. 8. Breakdown of CAPEX per MW capacity for (a) W1 high-current, (b) T1W1 and (c) T2W1.

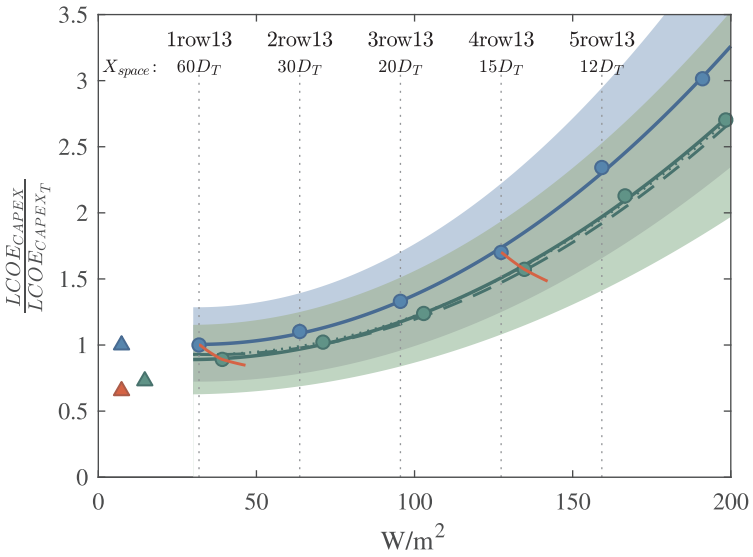

Fig. 10. $LCOE_{CAPEX}$ normalised by mean $LCOE_{CAPEX_T}$ versus capacity area density (W/m^2). Tidal-only (blues), co-located array with same tidal footprint (greens) based on upper and lower bound CAPEX estimates (shaded areas) and central CAPEX estimates (curves), with central estimate for shared supports of T2W1 (——), T1W1 (– – –) and separate supports (· · · ·). Triangle markers indicate cost for 3 MW wind turbine in low current (red), 3 MW tidal array (blue) and co-located farm with same 3 MW tidal array footprint and a T2W1 shared support (green). $LCOE_{CAPEX}$ for T2W1 support with varying wind turbine capacity as Table 8 (——) for 1row13 and 4row13 layouts only. Normalisation is with $LCOE_{CAPEX_T}$ = £88/MWh.

Table 8
Energy yield and $LCOE_{CAPEX}$ for varying wind turbine capacity between 0 and 6 MW for the 1row13 and 4row13 tidal array layouts. Results for 2T1W support with 1T1W shown in (brackets). $LCOE_{CAPEX_T}$ and $LCOE_{CAPEX_{arr}}$ represent the levelised capital costs of energy for a single tidal turbine and complete tidal-only array, respectively.

Wind capacity, MW	Wind energy yield, GWh	Ratio of wind/ tidal energy	$LCOE_{CAPEX}$	$LCOE_{CAPEX}$/ $LCOE_{CAPEX_T}$	$LCOE_{CAPEX}$/ $LCOE_{CAPEX_{arr}}$
1row13					
0	0	0	87.57 (87.57)	1.000 (1.000)	1.000 (1.000)
0.5	7.12	0.047	86.08 (88.77)	0.983 (1.014)	0.983 (1.014)
1	14.24	0.094	84.17 (86.74)	0.961 (0.991)	0.961 (0.991)
2	28.48	0.188	80.79 (83.16)	0.923 (0.950)	0.923 (0.950)
3	42.72	0.282	78.05 (80.24)	0.891 (0.916)	0.891 (0.916)
4	56.96	0.377	76.57 (78.62)	0.874 (0.898)	0.874 (0.898)
5	71.20	0.471	75.28 (77.20)	0.860 (0.882)	0.860 (0.882)
6	85.44	0.565	74.15 (75.95)	0.847 (0.867)	0.847 (0.867)
4row13					
0	0	0	148.93 (145.34)	1.701 (1.660)	0.990 (0.966)
0.5	7.12	0.020	147.08 (144.75)	1.680 (1.653)	0.977 (0.962)
1	14.24	0.040	145.05 (142.81)	1.656 (1.631)	0.964 (0.949)
2	28.48	0.080	141.21 (139.14)	1.613 (1.589)	0.938 (0.924)
3	42.72	0.120	137.72 (135.79)	1.573 (1.551)	0.915 (0.902)
4	56.96	0.160	134.92 (133.12)	1.541 (1.520)	0.896 (0.884)
5	71.20	0.200	132.30 (130.61)	1.511 (1.492)	0.880 (0.868)
6	85.44	0.240	129.85 (128.26)	1.483 (1.465)	0.863 (0.852)

rating (see Eq. (10)).

$$P = \frac{1}{2}\rho\alpha_s A C_P U^3 \tag{10}$$

where the power coefficient, C_P, is defined as the ratio of power generated by the turbine rotor relative to the power available in the flow through rotor swept area, A.

The tidal array layouts were kept identical to those used in all preceding analysis. In addition to the cost assumptions made earlier, three further clarifications should be noted:

- Wind turbine generator cost increases with installed wind turbine capacity.
- Foundation cost scales as cost/MW installed wind capacity. However a bottom limit is set such that the cost of foundation is not less than that required for a 3 MW wind turbine.
- Wind turbine tower cost is by cost/MW and so scales with wind turbine capacity.

In nearly all cases, cost savings are realised by adding a wind turbine to the array. Only for the T1W1 support with very small wind turbine capacities, approximately less than the capacity of each tidal turbine, does it become more expensive to add a wind turbine. This is not the case for the T2W1 support, effectively because two tidal turbines are mounted to the same support which represents a marginal cost saving over installing separate tidal turbines when no wind turbine is installed. The results show the greater the wind turbine capacity, the greater the cost saving. The greatest cost saving, around 15%, is for the largest capacity turbine. However, for a larger wind turbine, the required spacing of unit areas within a wind farm would increase.

6. Discussions

The focus of this study has been to investigate reductions in cost of energy from tidal stream sites by co-location of wind turbines with tidal stream turbines. This contrasts with adding tidal stream turbines to existing wind farms, where the typically low current speeds would result in the tidal turbines contributing very little extra energy yield; current speeds less than 2 m/s are not considered commercially viable for tidal stream energy [43]. The Pentland Inner Sound case study site considered is a particularly energetic tidal site where the tidal turbines contribute significantly to the overall co-located energy production. This was used to identify a ‘worst-case’ assessment for adding wind turbines to tidal arrays since other tidal sites with less energy potential will see a greater cost benefit from adding wind turbines, assuming similar wind climates.

The addition of tidal turbines to a wind turbine support platform increases the complexity of the platform and so this raises the question of the extent to which co-location may be of benefit for tidal sites with lower power potential. In this study, the rated capacity of tidal turbines on the shared platform is up to 66% of the wind turbine capacity, with

similar capacity factors for both the wind and tidal turbines. Hence, the tidal turbines contribute significantly to the energy yield from the co-located structure. In contrast, standalone tidal arrays are shown in Fig. 10 to only become cost-competitive against wind-only farms once lower-bound CAPEX estimates are realised for sparse array layouts. This suggests that for sites with less tidal stream energy potential and similar wind speed distribution, the cost of energy from tidal-only arrays will always be less economical than wind-only or co-located farms.

Comparison between co-located configurations has been presented on the basis of the levelised capital cost and the contribution from OPEX to the cost of energy has been neglected. Over the 20–25 year lifetime of an installation, the net present value of OPEX for wind farms and tidal stream arrays are estimated to be of similar magnitude to the total CAPEX [25]. This suggests that the levelised cost of energy is sensitive to OPEX for co-located farms as well and so this should be addressed in future studies. Approaches such as by [80] to map the sensitivity of levelised cost of energy to spatial variability of OPEX and [75] to calculate the temporal duration of suitable weather windows for site accessibility, could together be implemented to accurately assess OPEX for a co-located farm. A detailed review of vessels capable of conducting heavy-maintenance for co-located structures would also be necessary in order to assess whether new specialised vessels would be required for installation.

7. Conclusions

Co-location of a wind turbine with an array of tidal stream turbines has been investigated for the widely studied MeyGen site located in the Pentland Firth, UK. In all cases of practical interest, deployment of wind turbines always reduces the levelised capital cost of energy compared to a tidal array alone. Cost of energy decreases with increasing wind turbine capacity and for increasing streamwise tidal turbine spacing for arrays comprising either aligned rows of turbines or staggered arrays of turbines.

This reduction of cost of energy occurs due to an increase of energy yield and a reduction of capital cost per installed MW of capacity relative to isolated deployment of tidal turbines. Energy yield has been assessed using a wake superposition model in which the wakes of each turbine and the support structures are considered. Peak tidal energy yield for a unit area within an array was found for 4 rows of 13 turbines, with stream-wise and cross-stream spacing of X = 15 D_T and Y = 1.5 D_T, respectively. The addition of a single 3 MW wind turbine to this array increases net energy yield by around 11%, whereas for more sparsely populated tidal arrays, the wind turbine contributes an additional 28% energy yield for a unit area. Capital cost for the array is from the sum of cost centres from prior studies of representative tidal stream turbines and wind turbines. To estimate CAPEX cost centres for co-located devices, peak loads were established, with foundation costs scaled proportional to the increase in load. Despite loads for both T2W1 and T1W1 shared structures being 60% greater than for a wind turbine, the CAPEX centres per MW capacity were respectively 8% and 3% less than for a structure supporting a wind turbine only and 73% and 77% of a tidal-only device.

Co-location therefore offers the potential for 10–12% saving on $LCOE_{CAPEX}$ compared to a tidal-only array with same layout and low-packing density. This aligns with greatest capacity factor of the tidal turbines being achieved for low tidal turbine packing densities, for which minimal wake interactions occur. Future work is needed to assess vessel capability and the impact of operational expenditure on overall levelised cost of energy for co-located farms.

Acknowledgements

This work was jointly funded by the Engineering and Physical Sciences Research Council (Doctoral Training Partnership EP/K502947/1) and University of Manchester Alumni Research Impact Scholarship. The authors also thank Thomas Adcock (University of Oxford) who provided the ADCIRC tidal current data, and Philippe Gleizon (University of Highlands and Islands, Thurso) who provided the wave buoy data.

References

[1] European Environmental Agency. Renewable energy in Europe – recent growth and knock-on effects Tech. Rep.. Luxembourg: EEA; 2016.
[2] RenewableUK. Wind energy in the UK, state of the industry report. Tech. Rep.. 2015.
[3] Hassan GL Garrad. A guide to UK offshore wind operations and maintenance. Glasgow and London, UK: Scottish Enterprise and The Crown Estate; 2013. p. 42.
[4] Black and Veatch. Phase II – UK tidal stream energy resource assessment Tech. Rep.. Middlesex, UK: Black and Veatch Consulting Ltd.; 2005.
[5] Carbon Trust. AMEC environment & infrastructure UK limited, UK wave energy resource. Tech. Rep.. 2012.
[6] Bradley S. Wave Energy: Insights from the Energy Technologies Institute. Tech. Rep.. Loughborough, UK: ETI; 2015.
[7] ETI. Insights into tidal stream energy. Tech. Rep.. Loughborough, UK: Energy Technologies Institute; 2015.
[8] Tomey-Bozo N, Murphy J, Lewis T, Thomas G. A review and comparison of o shore oating conceptswith combined wind-wave energy. In: Proceedings of the 11th European wave and tidal energy conference; 2015,p. 1–8.
[9] Stoutenburg ED, Jenkins N, Jacobson MZ. Power output variations of co-located offshore wind turbines and wave energy converters in California. Renew Energy 2010;35(12):2781–91. https://doi.org/10.1016/j.renene.2010.04.033. [ISSN 09601481].
[10] Astariz S, Iglesias G. Enhancing wave energy competitiveness through co-located wind and wave energy farms. A review on the shadow effect. Energies 2015;8:7344–66. https://doi.org/10.3390/en8077344.
[11] MARINA. MARINA platform European union seventh framework programme (EU FP7) marine renewable integrated application grant agreement no. FP7-241402, 2010–2014 publishable summary. Tech. Rep.. EU FP7; 2014.
[12] Sudall D, Stansby P, Stallard T. Energy yield for collocated offshore wind and tidal stream farms. In: Proceedings of the EWEA offshore 2015; 2015, 1–10.
[13] Lande-Sudall D, Stallard T, Stansby P. Energy yield for co-located offshore wind and tidal stream farms. In: Soares C. (Ed.), Proceedings of the 2nd international conference on renewable energies offshore (RENEW). Lisbon, Portugal: Taylor and Francis; 2016.
[14] Lande-Sudall D, Stallard T, Stansby P. Co-located offshore wind and tidal stream turbines: assessment of energy yield and loading. Renew Energy, 2018, 118(c), https://doi.org/10.1016/j.renene.2017.10.063, ISSN 18790682.
[15] IEA, NEA. Projected costs of generating electricity 2010. Tech. Rep.. Paris, France: International Energy Agency and Nuclear Energy Agency; 2010.
[16] Allan G, Gilmartin M, McGregor P, Swales K. Levelised costs of Wave and Tidal energy in the UK: cost competitiveness and the importance of “banded” renewables obligation certificates. Energy Policy 2011;39(1):23–39. https://doi.org/10.1016/j.enpol.2010.08.029. [ISSN 03014215].
[17] Vazquez A, Iglesias G. Device interactions in reducing the cost of tidal stream energy. Energy Convers Manag 2015;97:428–38. https://doi.org/10.1016/j.enconman.2015.03.044. [ISSN 0196-8904].
[18] Myhr A, Bjerkseter C, Ågotnes A, Nygaard TA. Levelised cost of energy for offshore floating wind turbines in a life cycle perspective. Renew Energy 2014;66:714–28. https://doi.org/10.1016/j.renene.2014.01.017. [ISSN 09601481].
[19] Vazquez A, Iglesias G. Capital costs in tidal stream energy projects – a spatial approach. Energy 2016;107:215–26. https://doi.org/10.1016/j.energy.2016.03.123. [ISSN 03605442].
[20] Heptonstall P, Gross R, Greenacre P, Cockerill T. The cost of offshore wind: understanding the past and projecting the future. Energy Policy 2012;41:815–21. https://doi.org/10.1016/j.enpol.2011.11.050. [ISSN 03014215].
[21] BWEA, Hassan Garrad. UK Offshore Wind: Charting the Right Course. Tech. Rep.. 2009.
[22] Crown Estate. Offshore wind cost reduction-Pathways study; 2012, 88 pp.
[23] Catapult ORE. Cost reduction monitoring framework: summary report to the offshore wind programme board. Tech. Rep.. 2015.
[24] Carbon Trust. Accelerating marine energy. Tech. Rep.. London, UK: Carbon Trust; 2011.
[25] Ernst and Young. Cost of and financial support for wave, tidal stream and tidal range generation in the UK. Tech. Rep.. 2010.
[26] Krohn D, Woods M, Adams J, Valpy B, Jones F, Gardner P. Wave and tidal energy in the UK conquering challenges, generating growth. Tech. Rep.. London, UK: RenewableUK; 2013.
[27] Krohn S, Morthorst P-E, Awerbuch S. The economics of wind energy Tech. Rep.. EWEA; 2009.
[28] Ernst and Young. Cost of and financial support for offshore wind: a report for the department of energy and climate change. Tech. Rep.. 2009.
[29] Westwood D. Offshore wind asessment for Norway. Tech. Rep.. The Research Council of Norway; 2010.
[30] Carbon Trust. Value breakdown for the offshore wind sector. Renewables Advisory Board; 2010, 1–20.
[31] SI Ocean. Ocean energy: cost of energy and cost reduction opportunities. Tech. Rep.. 2013.
[32] Junginger M, Faaij A, Turkenburg W. Cost reduction prospects for offshore wind

farms. Wind Eng 2004;28(1):97–118. https://doi.org/10.1260/0309524041210847.
[33] MeyGen. MeyGen tidal energy project phase 1 environmental statement. Tech. Rep.. 2012.
[34] Stansby P, Stallard T. Fast optimisation of tidal stream turbine positions for power generation in small arrays with low blockage based on superposition of self-similar far-wake velocity deficit profiles. Renew Energy 2016;92:366–75. https://doi.org/10.1016/j.renene.2016.02.019. [ISSN 09601481].
[35] Stallard T. PerAWAT WG4 WP2 D2 design of equipment for scale model experiments. Tech. Rep.. Energy Technologies Institute; 2010.
[36] Jones IP, Wells aK, Starzmann R, Bischof S. CFD simulations of the TRITON tidal energy platform to analyse the surrounding flow pattern. In: Proceedings of the 11th European wave and tidal energy conference series; 2015, 1–10.
[37] Royal Haskoning. SeaGen Environmental Monitoring Programme Final Report. Tech. Rep. Edinburgh; 2011.
[38] McNaughton J. Turbulence modelling in the near-field of an axial flow tidal turbine using Code_Staturne [Ph.D. Thesis]. Manchester, UK: University of Manchester; 2013.
[39] Stallard T, Feng T, Stansby P. Experimental study of the mean wake of a tidal stream rotor in a shallow turbulent flow. J Fluids Struct 2014;54:235–46. https://doi.org/10.1016/j.jfluidstructs.2014.10.017. [ISSN 08899746].
[40] Shives M, Crawford C. Adapted two-equation turbulence closures for actuator disk RANS simulations of wind & tidal turbine wakes. Renew Energy 2016;92:273–92. https://doi.org/10.1016/j.renene.2016.02.026. [ISSN 18790682].
[41] ON E. Rampion offshore wind farm draft environmental statement. Tech. Rep.. 2012.
[42] Lande-Sudall D, Stallard T, Stansby P. Experimental study of the wakes due to tidal rotors and a shared cylindrical support. In: Proceedings of 12th European wave and tidal energy conference. Cork, Ireland; 2017.
[43] PMSS. Offshore renewables resource and development (ORRAD) project – technical report. Tech. Rep.. Hampshire, UK: Project Management Support Services Ltd.; 2010.
[44] Iyer AS, Couch S, Harrison G, Wallace R. Assessing long term tidal site characterisation using acoustic Doppler current profilers (ADCP). In: Proceedings of the 10th European wave and tidal energy conference. Aalborg, Denmark; 2013.
[45] Sellar B, Wakelam G. Characterisation of tidal flows at the European marine energy centre in the absence of ocean waves. Energies 2018;11(1):176. https://doi.org/10.3390/en11010176. [ISSN 1996-1073].
[46] Thomson J, Polagye B, Durgesh V, Richmond MC. Measurements of turbulence at two tidal energy sites in puget sound, WA. J Ocean Eng 2012;37(3):363–74. https://doi.org/10.1109/JOE.2012.2191656.
[47] Neill SP, Vögler A, Goward-Brown AJ, Baston S, Lewis MJ, Gillibrand PA, et al. The wave and tidal resource of Scotland. Renew Energy 2017;114:3–17. https://doi.org/10.1016/j.renene.2017.03.027. [ISSN 18790682].
[48] Easton MC, Harendza A, Woolf DK, Jackson AC. Characterisation of a tidal energy site: hydrodynamics and seabed structure. In: Proceedings of the 9th EWTEC conference. Southampton; 2011.
[49] Gillibrand PA, Walters RA, McIlvenny J. Numerical simulations of the effects of a tidal turbine array on near-bed velocity and local bed shear stress. Energies, 2016, 9(10), https://doi.org/10.3390/en9100852, ISSN 19961073.
[50] Martin-Short R, Hill J, Kramer S, Avdis A, Allison P. Tidal resource extraction in the Pentland Firth, UK: potential impacts on flow regime and sediment transport in the Inner Sound of Stroma. Renew Energy 2015;76:596–607. https://doi.org/10.1016/j.renene.2014.11.079. [ISSN 09601481].
[51] Waldman S, Bastón S, Nemalidinne R, Chatzirodou A, Venugopal V, Side J. Implementation of tidal turbines in MIKE 3 and Delft3D models of Pentland Firth & Orkney Waters. Ocean Coast Manag 2017;147:21–36. https://doi.org/10.1016/j.ocecoaman.2017.04.015. [ISSN 09645691].
[52] Adcock TAA, Draper S, Houlsby GT, Borthwick AGL, Serhadlıoğlu S. The available power from tidal stream turbines in the Pentland Firth. Proc R Soc A: Math Phys Eng Sci. 2013, https://doi.org/10.1098/rspa.2013.0072.
[53] Met Office. Operational Numerical Weather Prediction (NWP) Output from the UK Variable (UKV) Resolution Part of the Met Office Unified Model (UM); 2013.
[54] Blockley E, Siddorn J, Hackett B, McConnell N, Hines A. Product user manual for north-west shelf physical forecast product. Tech. Rep.. 2015.
[55] ECMWF, European Centre For Medium-range Weather Forecasts (ECMWF) re-analysis interim (ERA-Interim) model data., NCAS British Atmospheric Data Centre, 2009.
[56] Heathcote F, Vogel C, Willden RHJ. Design and operation of a 1 MW four turbine tidal fence. In: Soares CG (Ed.), Proceedings of the 2nd international conference on renewable energies offshore (RENEW). Lisbon, Portugal: Taylor and Francis, Lisbon; 2016.
[57] Kaiser MJ, Snyder B. Offshore wind energy installation and decommissioning cost estimation in the U.S. outer continental shelf. 2010. p. 340.
[58] Dicorato M, Forte G, Pisani M, Trovato M. Guidelines for assessment of investment cost for offshore wind generation. Renew Energy 2011;36(8):2043–51. https://doi.org/10.1016/j.renene.2011.01.003. [ISSN 09601481].
[59] Damiani R, Dykes K, Scott G. A comparison study of offshore wind support structures with monopiles and jackets for U.S. waters. J Phys: Conf Ser Sci Making Torque Wind (TORQUE), 2016, 753, https://doi.org/10.1088/1742-6596/753/9/092003, ISSN 17426596.
[60] Fischer J, Senet C. Oceanographic oberservations at FINO1 and the “Alpha Ventus” offshore wind farm. In: Proceedings of the 10th German wind energy conference. Bremen: DEWEK; 2010.
[61] O'Connor M, Burke D, Curtin T, Lewis T, Dalton G. Weather windows analysis incorporating wave height, wave period, wind speed and tidal current with relevance to deployment and maintenance of. In: Proceedings of the 4th...; 2012, 1–9.
[62] Mortensen NG. 46200 planning and development of wind farms: wind resource assessment using the WAsP software. Tech. Rep.. Roskilde: Technical University of Denmark; 2014.
[63] DNV. DNV-OS-J101 design of offshore wind turbine structures. 2013.
[64] Rienecker MM, Fenton JD, Fourier A. approximation method for steady water waves. J Fluid Mech 1981;104:119. https://doi.org/10.1017/S0022112081002851. [ISSN 0022-1120].
[65] Morison JR, Johnson JW, Brien MPO. Experimental studies of forces on piles. Coast Eng 1950:340–70.
[66] DNV. DNV-RP-C205 environmental conditions and environmental loads. 2014.
[67] Stansby PK, Devaney LC, Stallard TJ. Breaking wave loads on monopiles for offshore wind turbines and estimation of extreme overturning moment. IET Renew Power Gener 2013;7(5):514–20. https://doi.org/10.1049/iet-rpg.2012.0205. [ISSN 1752-1416].
[68] Fernandez-Rodriguez E, Stallard T, Stansby P. Experimental study of extreme thrust on a tidal stream rotor due to turbulent flow and with opposing waves. J Fluids Struct 2014;51:354–61. https://doi.org/10.1016/j.jfluidstructs.2014.09.012. [ISSN 08899746].
[69] 4C Offshore. Monopiles Support Structures, 2017.
[70] Maisondieu C, Johanning L, Weller S. Best practice report – installation procedures. Tech. Rep.. Marine Energy in Far Peripheral and Island Communities (MERiFIC); 2014.
[71] Stallard T, Dhedin JF, Saviot S, Noguera C. D7.4.1 procedures for estimating site accessibility & D7.4.2 appraisal of implications of site accessibility. Tech. Rep.. 2010.
[72] IT Power. Development, installation and testing of a large scale tidal current turbine. Tech. Rep.. DTI; 2005.
[73] Dudziak G, Waltham A, Barnes C. Marine energy supply chain survey. Tech. Rep.. Scottish Government; 2009.
[74] Argall R, Stephens R, Hindley S, Bates T, Torrens D, Heilmann R. HF4 – designing a DP vessel to support offshore renewables. In: Proceedings of the dynamic positioning conference. Marine Technology Society; 2014.
[75] Walker RT, Van Nieuwkoop-Mccall J, Johanning L, Parkinson RJ. Calculating weather windows: application to transit, installation and the implications on deployment success. Ocean Eng 2013;68:88–101. https://doi.org/10.1016/j.oceaneng.2013.04.015. [ISSN 00298018].
[76] Li L. Dynamic analysis of the installation of monopiles for offshore wind turbines [Ph.D. Thesis]. Trondheim, Norway: NTNU; 2016.
[77] Uraz E. Offshore wind turbine transportation & installation analyses [Ph.D. Thesis]. Visby, Sweden: Gotland University; 2011.
[78] Fraenkel P. Development and testing of marine current turbine’s SeaGen 1.2 MW tidal stream turbine. In: Proceedings of the 3rd international conference on ocean energy; 2010, 1–7.
[79] Andritz Hydro Hammerfest. ANDRITZ HYDRO Hammerfest Renewable energy from tidal currents; 2012, 1–12.
[80] Vazquez A, Iglesias G. LCOE (levelised cost of energy) mapping: a new geospatial tool for tidal stream energy. Energy 2015;91:192–201. https://doi.org/10.1016/j.energy.2015.08.012. [ISSN 03605442].